Non-Isochoric Plasticity Assessment for Accurate Crashworthiness CAE Analysis. Application to SAMP-1 and SAMP-Light.

Eduardo Martin-Santos[1], Lluis Martorell[1], Pablo Cruz[1], Megan Lobdell[2], Hubert Lobo[2]

[1]Applus IDIADA
[2]Applus DatapointLabs

1 Introduction

A deep understanding of advanced material plasticity and fracture is one of the cornerstones of mechanical engineering to overcome present and future challenges in the automotive industry with respect to lightweight multi-material body solutions.
The von Mises plasticity model is well-known and efficiently implemented in the various CAE solvers conventionally used in the automotive industry. One of the principal characteristics of the von Mises model is the assumption of isochoric plasticity (i.e. no change of volume is caused by yielding). The literature and experiments show that some materials, like extruded aluminium or polymers, exhibit non-isochoric plastic behaviour. Since this effect cannot be captured by the von Mises plasticity model, an optimal design for lightweight structural solutions is compromised.
In this paper, the authors propose a clear process to experimentally measure and assess how far uniaxially tested materials are from pure isochoric plastic behaviour. This process will be named Non-isochoric Plasticity Assessment (NPA). To illustrate the process, NPA will be applied to actual experimental results of representative automotive metals and thermoplastics. The application of this process will allow automotive CAE engineers to understand whether the von Mises plasticity model is appropriate for their analysis or if different material laws are required to accurately capture the material plastic behaviour. In addition to this, when fracture in the materials needs to be considered as a design parameter, the proper implementation of the plasticity mechanisms prior to failure becomes mandatory.
The paper also revisits fundamental plasticity theory concepts relevant for the use of non-isochoric plasticity material laws.
The overall approach described in this paper is validated for shell-based CAE models.

2 Non-isochoric plasticity theory background

A non-isochoric plasticity material law considers permanent dilation/compaction deformation of the material during plastic loading. This section provides a general description of the plasticity theory concepts required for the usage of non-isochoric plasticity material laws.

2.1 Stress and strain states relationship in non-isochoric plasticity

Any multiaxial stress state represented by the Cauchy stress tensor $\boldsymbol{\sigma}$ can be decomposed in its hydrostatic ($\boldsymbol{\sigma}_{\mathrm{H}}$) and deviatoric ($\boldsymbol{S}$) components (tensor magnitudes in compact notation denoted by bold font):

$$\boldsymbol{\sigma} = \mathbf{S} + \boldsymbol{\sigma}_{\mathrm{H}} \tag{1}$$

The hydrostatic stress tensor reads:

$$\boldsymbol{\sigma}_{\mathrm{H}} = \sigma_{\mathrm{m}}\boldsymbol{\delta} = -\mathrm{p}\boldsymbol{\delta} = \frac{1}{3}\mathrm{tr}[\boldsymbol{\sigma}]\boldsymbol{\delta} \tag{2}$$

being σ_{m} the mean stress, p the pressure ($\mathrm{p} = -\sigma_{\mathrm{m}}$) and $\boldsymbol{\delta}$ the second order identity tensor.
The multiaxial plastic strain state in its rate form $\dot{\boldsymbol{\varepsilon}}_{\mathrm{p}}$ developed by the multiaxial stress state $\boldsymbol{\sigma}$ can also be decomposed in its volumetric and deviatoric components, $\dot{\boldsymbol{\varepsilon}}_{\mathrm{pv}}$ and $\dot{\boldsymbol{\varepsilon}}_{\mathrm{pd}}$ respectively:

$$\dot{\boldsymbol{\varepsilon}}_{\mathrm{p}} = \dot{\boldsymbol{\varepsilon}}_{\mathrm{pd}} + \dot{\boldsymbol{\varepsilon}}_{\mathrm{pv}} \tag{3}$$

The volumetric plastic strain rate tensor $\dot{\boldsymbol{\varepsilon}}_{\mathrm{pv}}$ reads:

$$\dot{\boldsymbol{\varepsilon}}_{\mathrm{pv}} = \frac{1}{3}\dot{\varepsilon}_{\mathrm{pv}}\boldsymbol{\delta} = \frac{1}{3}\mathrm{tr}(\dot{\boldsymbol{\varepsilon}}_{\mathrm{p}})\boldsymbol{\delta} \tag{4}$$

being $\dot{\varepsilon}_{\mathrm{pv}}$ the volumetric plastic strain rate.

Stress and strains are expressed in their true form unless explicitly mentioned.
Based on the coaxial property of stress and strain states for an isotropic linear elastic material law (see [1] and [2]), the Cauchy stress tensor $\boldsymbol{\sigma}$ and the plastic strain rate tensor $\dot{\boldsymbol{\varepsilon}}_{\mathrm{p}}$ share the same principal directions space ($[\mathbf{I}, \mathbf{II}, \mathbf{III}]$ in the figure below). Therefore, $\boldsymbol{\sigma}$ and $\dot{\boldsymbol{\varepsilon}}_{\mathrm{p}}$ can be represented in the shared coaxial principal stress space. Additionally, the corresponding volumetric and deviatoric components of both $\boldsymbol{\sigma}$ and $\dot{\boldsymbol{\varepsilon}}_{\mathrm{p}}$ are colinear (i.e. parallel). The diagram below illustrates $\boldsymbol{\sigma}$ and $\dot{\boldsymbol{\varepsilon}}_{\mathrm{p}}$ and their volumetric-deviatoric components represented in the shared coaxial principal stress space in uniaxial conditions.

$$\begin{array}{ccccc} \boldsymbol{\sigma} & = & \boldsymbol{\sigma}_{\mathrm{H}} & + & \mathbf{S} \\ \Updownarrow & & \Updownarrow & & \Updownarrow \\ \dot{\boldsymbol{\varepsilon}}_{\mathrm{p}} & = & \dot{\boldsymbol{\varepsilon}}_{\mathrm{pv}} & + & \dot{\boldsymbol{\varepsilon}}_{\mathrm{pd}} \end{array} \tag{5}$$

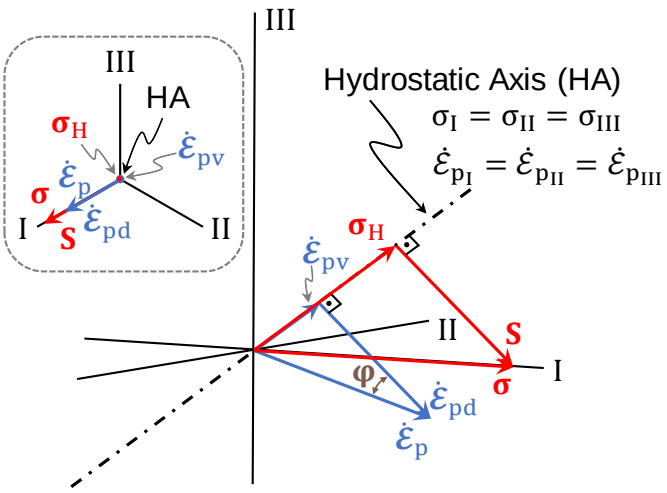

The dilation angle φ defines the ratio between volumetric and deviatoric plastic strain rates developed during plastic loading (as shown in the figures above and below):

- $\varphi > 0º$ corresponds to plastic dilation (i.e. $\dot{\varepsilon}_{\mathrm{pv}} > 0$)
- $\varphi = 0º$ corresponds to isochoric plasticity or pure shear plastic loading
- $\varphi < 0º$ corresponds to plastic compaction (i.e. $\dot{\varepsilon}_{\mathrm{pv}} < 0$)

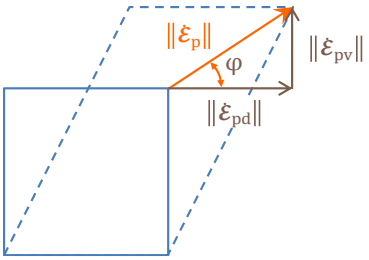

The dilation angle φ is defined by the volumetric and deviatoric plastic strain rate tensor modules, $\|\dot{\boldsymbol{\varepsilon}}_{\mathrm{pv}}\|$ and $\|\dot{\boldsymbol{\varepsilon}}_{\mathrm{pd}}\|$ respectively:

$$\mathrm{tg}\varphi = \frac{\|\dot{\boldsymbol{\varepsilon}}_{\mathrm{pv}}\|}{\|\dot{\boldsymbol{\varepsilon}}_{\mathrm{pd}}\|} \tag{6}$$

with,

$$\|\dot{\boldsymbol{\varepsilon}}_{\mathrm{pv}}\| = \sqrt{\dot{\boldsymbol{\varepsilon}}_{\mathrm{pv}} : \dot{\boldsymbol{\varepsilon}}_{\mathrm{pv}}} \quad \& \quad \|\dot{\boldsymbol{\varepsilon}}_{\mathrm{pd}}\| = \sqrt{\dot{\boldsymbol{\varepsilon}}_{\mathrm{pd}} : \dot{\boldsymbol{\varepsilon}}_{\mathrm{pd}}} \tag{7}$$

Regarding the plastic strain evolution:

- volumetric plastic strain states can only be developed by hydrostatic stress states
- deviatoric (shear) plastic strain states can only be developed by deviatoric stress states
- the total plastic strain state is obtained composing the corresponding volumetric and deviatoric components (i.e. $\dot{\boldsymbol{\varepsilon}}_{\mathrm{p}} = \dot{\boldsymbol{\varepsilon}}_{\mathrm{pd}} + \dot{\boldsymbol{\varepsilon}}_{\mathrm{pv}}$)
- the total plastic strain rate ($\dot{\boldsymbol{\varepsilon}}_{\mathrm{p}}$) growth direction is defined by the dilation angle φ. Thus, the dilation angle plays a relevant role in the flow rule definition of the non-isochoric plasticity material laws where $\dot{\boldsymbol{\varepsilon}}_{\mathrm{pv}}$ is not null (i.e. $\dot{\boldsymbol{\varepsilon}}_{\mathrm{pv}} \neq \mathbf{0}$)

The characterization of the plastic behaviour of a material that exhibits volumetric plastic strain while yielding will require the experimental measurement for a material property related to the dilation angle. As it will be shown below, it turns out that this material property is the plastic Poisson's ratio.
The deviatoric plastic strain rate tensor module $\|\dot{\boldsymbol{\varepsilon}}_{\mathrm{pd}}\|$ can be expressed as a function of the equivalent plastic strain rate $\dot{\varepsilon}_{\mathrm{peq}}$:

$$\dot{\varepsilon}_{\mathrm{peq}} \overset{\text{def}}{=} \sqrt{\frac{2}{3}\,\dot{\boldsymbol{\varepsilon}}_{\mathrm{pd}} : \dot{\boldsymbol{\varepsilon}}_{\mathrm{pd}}} = \sqrt{2/3}\,\|\dot{\boldsymbol{\varepsilon}}_{\mathrm{pd}}\| \quad \Rightarrow \quad \|\dot{\boldsymbol{\varepsilon}}_{\mathrm{pd}}\| = \sqrt{3/2}\,\dot{\varepsilon}_{\mathrm{peq}} \tag{8}$$

The volumetric plastic strain rate tensor module can be expressed as a function of the volumetric plastic strain rate $\dot{\varepsilon}_{\mathrm{pv}}$:

$$\dot{\boldsymbol{\varepsilon}}_{\mathrm{pv}} = \frac{1}{3}\dot{\varepsilon}_{\mathrm{pv}}\boldsymbol{\delta} \quad \Rightarrow \quad \|\dot{\boldsymbol{\varepsilon}}_{\mathrm{pv}}\| = \frac{1}{\sqrt{3}}|\dot{\varepsilon}_{\mathrm{pv}}| \tag{9}$$

Therefore, without loss of generality, the expression of the dilation angle can be defined as a function of both the equivalent and the volumetric plastic strain rates (dilation/compaction sign enforced by the latter):

$$\mathrm{tg}\varphi = \frac{\sqrt{2}}{3}\frac{\dot{\varepsilon}_{\mathrm{pv}}}{\dot{\varepsilon}_{\mathrm{peq}}} \tag{10}$$

Regarding the material plastic dilation and compaction behaviour, the following concepts are remarked:

- Only stress states involving hydrostatic tension ($\sigma_{\mathrm{m}} > 0$) can develop plastic dilation when yielding
- Only stress states involving hydrostatic compression ($\sigma_{\mathrm{m}} < 0$) can develop plastic compaction when yielding

Due to the homogeneous nature of the hydrostatic stress, if a volumetric plastic dilation material property is experimentally measured for one stress state involving hydrostatic tension ($\sigma_{\mathrm{m}} > 0$), the characterization of the rest of hydrostatic tension stress states can be based on the experimentally measured property plus the stress state influence (i.e. triaxiality influence). In this paper, the material volumetric plastic dilation behaviour is characterized by means of the experimental measurement of the plastic Poisson's ratio in uniaxial tension conditions. Volumetric plastic compaction is not in the scope of this paper.
The general dilation angle expression (Eq. 10) particularized for the uniaxial tension case reads:

$$\mathrm{tg}\varphi_{\mathrm{ut}} = \frac{\sqrt{2}}{3}\frac{\dot{\varepsilon}_{\mathrm{pv}}^{\mathrm{ut}}}{\dot{\varepsilon}_{\mathrm{peq}}^{\mathrm{ut}}} \tag{11}$$

Let $\dot{\boldsymbol{\varepsilon}}_{\mathrm{p}}^{\mathrm{ut}}$ be the characteristic plastic strain rate tensor under uniaxial tension conditions, $\dot{\varepsilon}_{\mathrm{p}}^{\mathrm{ut}}$ the uniaxial tension plastic strain rate and ν_{p} the material plastic Poisson's ratio exhibited during uniaxial tension yielding:

$$\dot{\boldsymbol{\varepsilon}}_{\mathrm{p}}^{\mathrm{ut}} = \begin{bmatrix} \dot{\varepsilon}_{\mathrm{p}}^{\mathrm{ut}} & 0 & 0 \\ 0 & -\nu_{\mathrm{p}}\dot{\varepsilon}_{\mathrm{p}}^{\mathrm{ut}} & 0 \\ 0 & 0 & -\nu_{\mathrm{p}}\dot{\varepsilon}_{\mathrm{p}}^{\mathrm{ut}} \end{bmatrix} \tag{12}$$

The dilation angle obtained from the characteristic plastic strain rate tensor in the uniaxial tension case reads:

$$\mathrm{tg}\varphi_{\mathrm{ut}} = \frac{\left\|\dot{\boldsymbol{\varepsilon}}_{\mathrm{pv}}^{\mathrm{ut}}\right\|}{\left\|\dot{\boldsymbol{\varepsilon}}_{\mathrm{pd}}^{\mathrm{ut}}\right\|} = \frac{1}{\sqrt{2}}\frac{1-2\nu_{\mathrm{p}}}{1+\nu_{\mathrm{p}}} \tag{13}$$

The expression above shows the direct relationship between the dilation angle and the plastic Poisson's ratio in the uniaxial stress case. Therefore, the volumetric plastic dilation can be characterized by means of the experimental measurement of the plastic Poisson's ratio in uniaxial tension conditions plus the stress state influence.

2.2 Plastic Poisson's ratio in uniaxial tension conditions

As explained above, the volumetric plastic dilation will be characterized by means of the experimental measurement of the plastic Poisson's ratio from uniaxial tension tests.
The volumetric plastic strain rate in uniaxial tension conditions $\dot{\varepsilon}_{\mathrm{pv}}^{\mathrm{ut}}$ obtained from $\dot{\boldsymbol{\varepsilon}}_{\mathrm{p}}^{\mathrm{ut}}$ reads:

$$\dot{\varepsilon}_{\mathrm{pv}}^{\mathrm{ut}} = \mathrm{tr}\left(\dot{\boldsymbol{\varepsilon}}_{\mathrm{p}}^{\mathrm{ut}}\right) = \left(1-2\nu_{\mathrm{p}}\right)\dot{\boldsymbol{\varepsilon}}_{\mathrm{p}}^{\mathrm{ut}} \tag{14}$$

Note that applying the isochoric plasticity assumption into $\dot{\boldsymbol{\varepsilon}}_{\mathrm{p}}^{\mathrm{ut}}$ implies setting a constant plastic Poisson's ratio ν_{p} equal to 0.5. Then, $\dot{\varepsilon}_{\mathrm{pv}}^{\mathrm{ut}} = 0$.
Using the volumetric plastic strain rate expression above (Eq. 14), the plastic Poisson's ratio can be then expressed as:

$$\nu_{\mathrm{p}} = \frac{1}{2}\left(1 - \frac{\dot{\varepsilon}_{\mathrm{pv}}^{\mathrm{ut}}}{\dot{\varepsilon}_{\mathrm{p}}^{\mathrm{ut}}}\right) \tag{15}$$

The equivalent plastic strain rate in uniaxial tension conditions obtained from $\dot{\boldsymbol{\varepsilon}}_{\mathrm{p}}^{\mathrm{ut}}$ reads:

$$\dot{\varepsilon}_{\mathrm{peq}}^{\mathrm{ut}} = \sqrt{\frac{2}{3}\,\dot{\boldsymbol{\varepsilon}}_{\mathrm{pd}}^{\mathrm{ut}} : \dot{\boldsymbol{\varepsilon}}_{\mathrm{pd}}^{\mathrm{ut}}} = \frac{2}{3}\left(1+\nu_{\mathrm{p}}\right)\dot{\varepsilon}_{\mathrm{p}}^{\mathrm{ut}} \tag{16}$$

Furthermore, an additional expression of the equivalent plastic strain rate in uniaxial tension conditions $\dot{\varepsilon}_{\mathrm{peq}}^{\mathrm{ut}}$ can be obtained combining equations (15) and (16). In other words,

$$\dot{\varepsilon}_{\mathrm{peq}}^{\mathrm{ut}} = \dot{\varepsilon}_{\mathrm{p}}^{\mathrm{ut}} - \frac{1}{3}\dot{\varepsilon}_{\mathrm{pv}}^{\mathrm{ut}} \tag{17}$$

2.3 Plastic Poisson's ratio measured from uniaxial tension experiments

Assuming isotropic linear elastic material behaviour, the material law can be expressed as:

$$\boldsymbol{\sigma} = \mathbf{D}_{\mathrm{e}} : \boldsymbol{\varepsilon}_{\mathrm{e}} = 2\mathrm{G}\boldsymbol{\varepsilon}_{\mathrm{ed}} + 3\mathrm{K}\boldsymbol{\varepsilon}_{\mathrm{ev}} \tag{18}$$

being $\boldsymbol{\sigma}$ the Cauchy stress tensor, $\mathbf{D}_e$ the Hooke elasticity tensor, $\boldsymbol{\mathcal{E}}_e$ the elastic strain tensor, $\boldsymbol{\mathcal{E}}_{ed}$ the deviatoric elastic strain tensor, $\boldsymbol{\mathcal{E}}_{ev}$ the volumetric elastic strain tensor ($\dot{\boldsymbol{\mathcal{E}}}_{ev} = \frac{1}{3}\dot{\mathcal{E}}_{ev}\boldsymbol{\delta} = \frac{1}{3}\mathrm{tr}(\dot{\boldsymbol{\mathcal{E}}}_e)\boldsymbol{\delta}$), G the shear modulus and K the bulk modulus.
Direct comparison of the isotropic linear elastic material law and the volumetric-deviatoric stress tensor split leads to:

$$\boldsymbol{\sigma} = \mathbf{S} + \boldsymbol{\sigma}_H = 2G\boldsymbol{\mathcal{E}}_{ed} + 3K\boldsymbol{\mathcal{E}}_{ev} \Rightarrow \begin{cases} \mathbf{S} = 2G\boldsymbol{\mathcal{E}}_{ed} \\ \boldsymbol{\sigma}_H = 3K\boldsymbol{\mathcal{E}}_{ev} \end{cases} \tag{19}$$

Based on the hydrostatic component comparison, the relation between the mean stress σ_m and the elastic volumetric strain $\mathcal{E}_{ev}$ can be expressed as:

$$\boldsymbol{\sigma}_H = 3K\boldsymbol{\mathcal{E}}_{ev} \;\Rightarrow\; \sigma_m\boldsymbol{\delta} = K\mathcal{E}_{ev}\boldsymbol{\delta} \;\Rightarrow\; \sigma_m = K\mathcal{E}_{ev} \;\Rightarrow\; \mathcal{E}_{ev} = \frac{\sigma_m}{K} \tag{20}$$

The uniaxial tension stress tensor and the corresponding mean stress read:

$$\boldsymbol{\sigma}_{ut} = \begin{bmatrix} \sigma_{ut} & 0 & 0 \\ 0 & 0 & 0 \\ 0 & 0 & 0 \end{bmatrix} \qquad \& \qquad \sigma_m^{ut} = \frac{1}{3}\mathrm{tr}[\boldsymbol{\sigma}_{ut}] = \frac{1}{3}\sigma_{ut} \tag{21}$$

Uniaxial tension true total strains ($\mathcal{E}_i^{ut}$) from engineering strains (e_i) read:

$$\mathcal{E}_i^{ut} = \ln(1 + e_i) \quad , \quad i = 1,2,3 \tag{22}$$

with direction 1 parallel to the specimen longitudinal direction, direction 2 parallel to the specimen transversal direction and direction 3 parallel to the specimen thickness direction.
In uniaxial tension conditions the total volumetric strain reads:

$$\mathcal{E}_v^{ut} = \mathcal{E}_1^{ut} + \mathcal{E}_2^{ut} + \mathcal{E}_3^{ut} \tag{23}$$

In order to have all the needed experimental data for this methodology, the uniaxial tension tests will require the use of digital image correlation (DIC) tools for the determination of the experimental strain distribution.
If the measurement of the strain in the thickness direction is not available from experiments, it can be assumed that strain in the thickness direction e_3^{ut} is similar to the transversal strain e_2^{ut}.
The uniaxial true stress reads:

$$\sigma_{ut} = \frac{F_{ut}}{A_0(1 + e_2^{ut})(1 + e_3^{ut})} \tag{24}$$

with F_{ut} the uniaxial tension force, A_0 the original specimen cross section and e_2^{ut} and e_3^{ut} the engineering strains in the transverse and thickness direction respectively.
The uniaxial tension longitudinal plastic strain reads:

$$\mathcal{E}_p^{ut} = \mathcal{E}_1^{ut} - \frac{\sigma_{ut}}{E} \tag{25}$$

being E the material's Young's modulus and $\mathcal{E}_1^{ut}$ the total longitudinal strain.
Elastoplastic additive decomposition of the total volumetric strain $\mathcal{E}_v^{ut}$ reads:

$$\mathcal{E}_v^{ut} = \mathcal{E}_{ev}^{ut} + \mathcal{E}_{pv}^{ut} \tag{26}$$

The volumetric plastic strain $\mathcal{E}_{pv}^{ut}$ can be directly obtained from experimental results subtracting the elastic volumetric strain from the total volumetric strain.

$$\varepsilon_v^{ut} = \varepsilon_{ev}^{ut} + \varepsilon_{pv}^{ut}$$
$$\varepsilon_{ev}^{ut} = \frac{\sigma_m^{ut}}{K}$$
$$\Downarrow$$
$$\varepsilon_{pv}^{ut} = \varepsilon_v^{ut} - \frac{\sigma_m^{ut}}{K} \quad (27)$$
$$\text{with} \quad \sigma_m^{ut} = \frac{1}{3}\sigma_{ut}$$

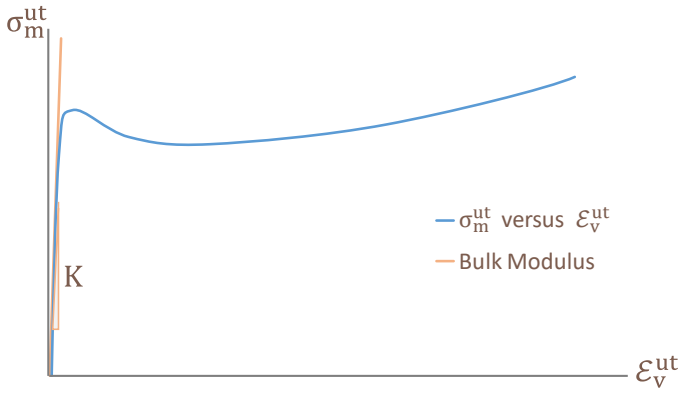

Mean Stress σ_m^{ut} vs. Total Volumetric Strain ε_v^{ut} (Uniaxial Tension)

Consequently, the plastic Poisson's ratio can be directly assessed from the uniaxial tension experimental results applying the expression:

$$\nu_p = \frac{1}{2}\left(1 - \frac{\varepsilon_{pv}^{ut}}{\varepsilon_p^{ut}}\right) \quad (28)$$

The plastic Poisson's ratio measured from the uniaxial tension experiments plus the stress state influence will define the volumetric plastic dilation for the rest of stress states involving hydrostatic tension (i.e. with $\sigma_m > 0$).

2.4 Plastic work consistency in non-isochoric plasticity

Isochoric plasticity assumes that only the stresses that generate shape distortion (i.e. deviatoric stresses) develop plastic strains in the material while yielding. Consequently, it is also assumed that the material cannot develop volumetric plastic strains in this regime. These assumptions lead to the definition of a single pair of energetic conjugates to satisfy the required plastic work consistency in the von Mises plasticity model. Then, the volumetric strain is considered as purely elastic in the material's behaviour. The isochoric pair of deviatoric energetic conjugates are the well-known equivalent von Mises stress σ_{vm} and the equivalent plastic strain ε_{peq} defined as:

$$\sigma_{vm} = \sqrt{\frac{3}{2}\mathbf{S}:\mathbf{S}} \quad \& \quad \varepsilon_{peq} = \sqrt{\frac{2}{3}\boldsymbol{\varepsilon}_{pd}:\boldsymbol{\varepsilon}_{pd}} \quad (29)$$

Please note that in isochoric plasticity $\boldsymbol{\varepsilon}_p = \boldsymbol{\varepsilon}_{pd}$ because $\boldsymbol{\varepsilon}_{pv} = \mathbf{0}$.
Non-isochoric plasticity requires the consideration of volumetric energetic conjugates in the plastic work consistency. Thus, it is necessary to define the equivalent volumetric stress σ_{eq}^{vol} and the equivalent volumetric plastic strain ε_{peq}^{vol}.
The plastic work concept ($\dot{W}_p$ in its rate form) provides consistency to the material plasticity model by associating multiaxial stress states ($\boldsymbol{\sigma}$) and multiaxial plastic strain rate states ($\dot{\boldsymbol{\varepsilon}}_p$) to the corresponding scalar equivalent magnitudes at both deviatoric and volumetric level. In other words,

$$\dot{W}_p = \sigma_{vm} \cdot \dot{\varepsilon}_{peq} + \sigma_{eq}^{vol} \cdot \dot{\varepsilon}_{peq}^{vol} \quad (30)$$

$$\dot{W}_p = \boldsymbol{\sigma}:\dot{\boldsymbol{\varepsilon}}_p = (\mathbf{S} + \boldsymbol{\sigma}_H):\left(\dot{\boldsymbol{\varepsilon}}_{pd} + \dot{\boldsymbol{\varepsilon}}_{pv}\right) \quad (31)$$

Expanding the plastic work rate in tensorial form (Eq. 31) reads:

$$\dot{W}_p = \boldsymbol{\sigma}: \dot{\boldsymbol{\varepsilon}}_p = \mathbf{S}: \dot{\boldsymbol{\varepsilon}}_{pd} + \mathbf{S}: \dot{\boldsymbol{\varepsilon}}_{pv} + \boldsymbol{\sigma}_H: \dot{\boldsymbol{\varepsilon}}_{pd} + \boldsymbol{\sigma}_H: \dot{\boldsymbol{\varepsilon}}_{pv} \tag{32}$$

The inner product (i.e. double contraction operator ":") between two coaxial symmetric second order tensors can be understood as the scalar product of the corresponding principal vectors represented in the shared coaxial principal stress space.
Therefore,

- $\mathbf{S}: \dot{\boldsymbol{\varepsilon}}_{pv} = 0$ because $\mathbf{S}$ and $\dot{\boldsymbol{\varepsilon}}_{pv}$ are perpendicular
- $\boldsymbol{\sigma}_H: \dot{\boldsymbol{\varepsilon}}_{pd} = 0$ because $\boldsymbol{\sigma}_H$ and $\dot{\boldsymbol{\varepsilon}}_{pd}$ are perpendicular

Consequently,

$$\dot{W}_p = \boldsymbol{\sigma}: \dot{\boldsymbol{\varepsilon}}_p = \mathbf{S}: \dot{\boldsymbol{\varepsilon}}_{pd} + \boldsymbol{\sigma}_H: \dot{\boldsymbol{\varepsilon}}_{pv} = \dot{W}_{pd} + \dot{W}_{pv}$$

$$\left.\begin{aligned} \boldsymbol{\sigma}_H &= \sigma_m \boldsymbol{\delta} \\ \dot{\boldsymbol{\varepsilon}}_{pv} &= \frac{1}{3}\dot{\varepsilon}_{pv}\boldsymbol{\delta} \end{aligned}\right\} \Rightarrow \dot{W}_{pv} = \boldsymbol{\sigma}_H: \dot{\boldsymbol{\varepsilon}}_{pv} = \sigma_m \frac{1}{3}\dot{\varepsilon}_{pv}\, \boldsymbol{\delta}: \boldsymbol{\delta} = \sigma_m \dot{\varepsilon}_{pv} \tag{33}$$

hence,

$$\dot{W}_{pv} = \sigma_{eq}^{vol} \cdot \dot{\varepsilon}_{peq}^{vol} = \sigma_m \cdot \dot{\varepsilon}_{pv} \Rightarrow \begin{cases} \sigma_{eq}^{vol} = \sigma_m \\ \varepsilon_{peq}^{vol} = \varepsilon_{pv} \end{cases} \tag{34}$$

It turns out that the equivalent volumetric stress is the mean stress and the equivalent volumetric plastic strain is the volumetric plastic strain. Thus,

$$\dot{W}_p = \dot{W}_{pd} + \dot{W}_{pv} = \sigma_{vm} \cdot \dot{\varepsilon}_{peq} + \sigma_m \cdot \dot{\varepsilon}_{pv} \tag{35}$$

Each pair of energetic conjugates represent a different plastic mechanism exhibited by the material while yielding:

- σ_{vm} and ε_{peq} represent the distortional (shear) yielding
- σ_m and ε_{pv} represent the plastic dilation and compaction yielding

Thus, as discussed in section 2.3, the material plastic dilation/compaction behaviour can be assessed and quantified considering the relationships between the volumetric and deviatoric plastic mechanisms represented by their energetic conjugates.
The material energy absorption computed in crashworthiness CAE analysis includes both volumetric and deviatoric plastic work when a non-isochoric plasticity material law is used.

3 Non-isochoric Plasticity Assessment (NPA)

In this section, NPA is illustrated applying the assessment to standard materials used in the automotive industry: a high-strength steel, an extruded aluminium and a thermoplastic.
The main objective of NPA is to assess the non-isochoric material's behaviour. This is performed by means of obtaining the plastic Poisson's ratio from uniaxial tension experiments and comparing it to the isochoric assumption of $\nu_p = 0.5$.
The plot below shows the plastic Poisson's ratio versus the longitudinal plastic strain, both directly obtained from uniaxial tension experimental measurements.

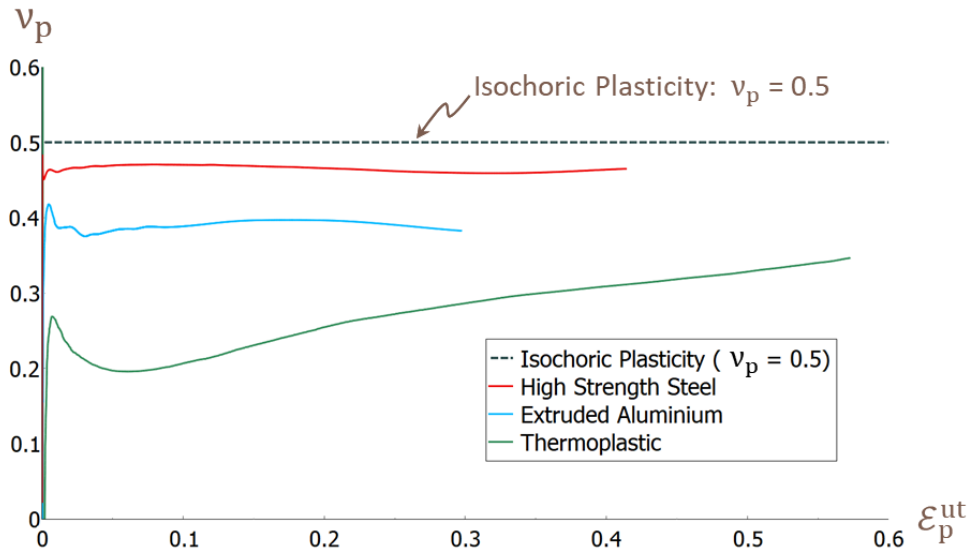

Uniaxial tension plastic Poisson's ratio ν_p vs. Longitudinal plastic strain ε_p^{ut}

NPA above clearly shows that:

- For the analysed high-strength steel, the application of von Mises plasticity is acceptable. In this case there would be some room for accuracy improvement if non-isochoric plasticity is considered, but the efforts may not be translated into significant enhancements.
- For the analysed extruded aluminium, the deviation from isochoric plasticity is higher than 20%. Therefore, it is recommended to migrate to a material law that incorporates non-isochoric plasticity. This recommendation is especially relevant for extruded aluminium where the typical tension-compression yield stress asymmetry (i.e. strength differential) cannot be captured by pressure-insensitive yield stress surfaces (like the von Mises yield stress surface). The plastic Poisson's ratio in this case could be considered constant with respect to the evolution of the plastic strain.
- For the analysed thermoplastic, the consideration of non-isochoric plasticity is a must in order to obtain the necessary CAE accuracy levels to reach an efficient lightweight design. In this case the variation of the plastic Poisson's ratio with respect to evolution of the longitudinal plastic strain should also be considered in the material law.

It is important to recall that in the von Mises plasticity model, volumetric stresses can only generate elastic volumetric strains. In materials showing a relevant part of volumetric plastic strain, this mechanism drives the material plastic dilation and the subsequent degradation of the material properties caused by micro-voids nucleation and growth. Plastic dilation is normally the precursor of material failure, finally caused by shear mechanisms (deviatoric plastic strains) when the coalescence of these micro-voids occurs in the shear bands. Therefore, in order to apply a controlled-fracture driven body design approach, accurate crashworthiness CAE analysis requires the use of advanced plasticity material laws to achieve lightweight and efficient body solutions.
The figures below show thermoplastic (left) and aluminium (right) broken specimens, tested in quasi-static conditions. In both cases, specimens exhibit volumetric plastic dilation (micro-voids nucleation, growth and coalescence) in the centre of the fracture surface and shear plastic bands and fracture outside the core region. In the case of the thermoplastic, crazing and fibrillation can also be seen.

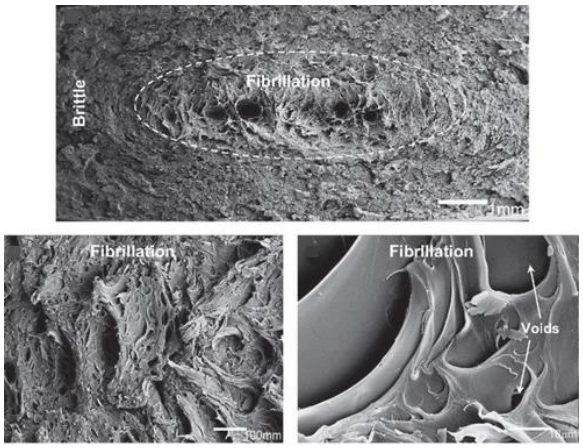

2004 Hadal et al. [3]
Thermoplastic plasticity and fracture

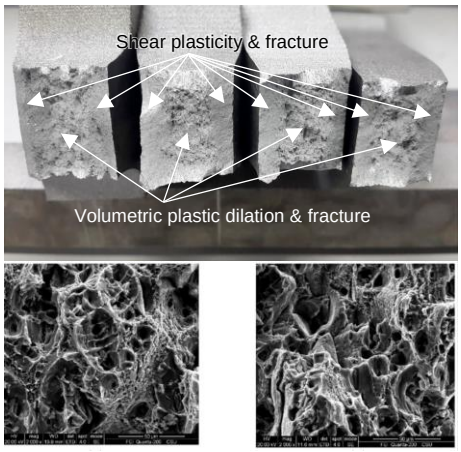

2017 Chen et al. [4]
Extruded aluminium plasticity and fracture

Generally, regarding ductile linear elastic isotropic materials, we can define two material families:

- materials where the void nucleation starts with the fracture onset (e.g. most steels);
- and materials where the void nucleation and growth start with the plasticity onset (e.g. thermoplastics and extruded aluminium)

For the first family of materials, void nucleation, growth and coalescence can be completely implemented in the material fracture constitutive model because there is no volumetric plastic strain history before the fracture onset.
For the second family of materials, void nucleation and growth need to be implemented in the material plasticity law:

- for capturing the actual material plastic behaviour (i.e. volumetric and shear yielding);
- and for providing to the fracture model the volumetric plastic strain history before the fracture onset to accurately predict the void growth and coalescence in the material fracture region.

It is for these reasons that non-isochoric plasticity material laws are required to accurately capture the material fracture in materials like thermoplastics and extruded aluminium that exhibit volumetric plastic dilation (i.e. void nucleation and growth) from the beginning of yielding. The main objective is to build up a triaxiality-based ductile failure envelope driven by both volumetric & deviatoric plastic mechanisms.

4 SAMP-1 and SAMP-Light: Non-isochoric plasticity material laws

NPA provides CAE engineers a clear process to understand when the isochoric plasticity assumption is acceptable. Based on the authors' experience, alternative material laws should be investigated whenever the deviation from the isochoric plasticity assumption is higher than 20%. When this occurs, taking as reference LS-Dyna CAE solver, the use of laws considering non-isochoric behaviour, such as SAMP-1 (**`*MAT_187`**) or SAMP-Light (**`*MAT_187L`**) are recommended.
SAMP-1 and SAMP-Light include all necessary features to capture the material non-isochoric plastic behaviour together with a pressure-dependent yield surface able to properly represent tension-compression yield stress asymmetries.
SAMP-1 and SAMP-Light consider the same non-associated flow rule. Thus, the main contents of this section are valid for both material cards.
All CAE results shown in this section come from shell-based FE-models.

4.1 SAMP-1 and SAMP-Light dilation angle & plastic Poisson's ratio

In SAMP-1 the material volumetric plastic dilation can be characterized under uniaxial tension and compression plastic loading conditions.
The objective of this section is to review how the experimentally measured material plastic Poisson's ratio is incorporated into the SAMP-1 plasticity model. The dilation angle consistency will be the non-isochoric plasticity theory concept used to incorporate the plastic Poisson's ratio into both SAMP-1 and SAMP-Light material laws.
In SAMP-1 non-associated flow rule (FR superscript), the volumetric plastic dilation is controlled in the flow tensor $\mathbf{N}$ by means of the dilation angle coefficient α that is defined in the plastic potential g. SAMP-1 and SAMP-Light flow rule reads:

$$\dot{\boldsymbol{\varepsilon}}_p^{FR} = \dot{\lambda}\,\mathbf{N} = \dot{\lambda}\frac{\partial g}{\partial \boldsymbol{\sigma}} \qquad \text{with} \qquad g \overset{\text{def}}{=} \sqrt{\sigma_{vm}^2 + \alpha p^2} \tag{36}$$

where λ is a nonnegative scalar associated with the evolution of the plastic deformation process also known as the plastic multiplier.
The flow tensor $\mathbf{N}$ is defined as the normal of the flow rule plastic potential surface g in the coaxial principal stress space:

$$\mathbf{N} = \nabla g = \frac{\partial g}{\partial \boldsymbol{\sigma}} = \frac{3}{2g}\mathbf{S} + \frac{\alpha}{3g}\boldsymbol{\sigma}_H \tag{37}$$

SAMP-1 flow tensor $\mathbf{N}$ and the quadratic yield surface f are represented below in the σ_{vm}-p meridian plane from the coaxial principal stress space together with the dilation angle depicted in uniaxial tension conditions.

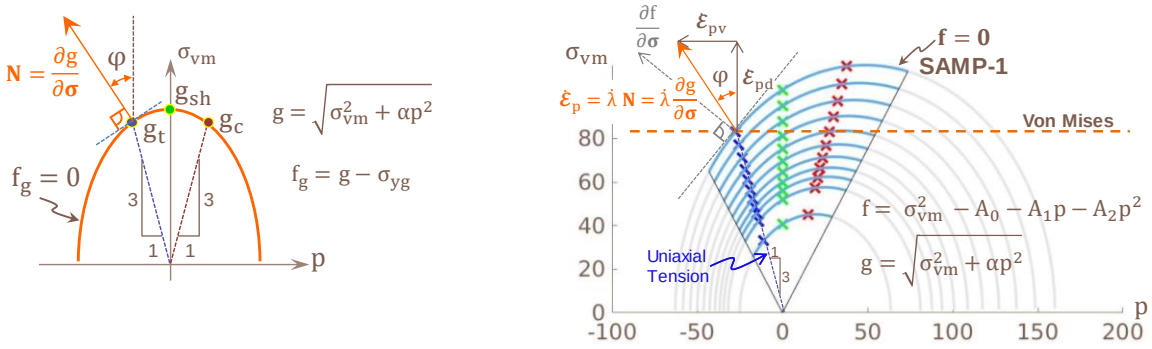

The flow tensor $\mathbf{N}$ and the dilation angle φ both define the growth direction of the plastic strain rate tensor $\dot{\boldsymbol{\varepsilon}}_p$.

The general dilation angle expression obtained from the flow rule plastic strain rate tensor ($\dot{\boldsymbol{\varepsilon}}_p^{FR}$) reads:

$$tg\varphi^{FR} = \frac{\left\|\dot{\boldsymbol{\varepsilon}}_{pv}^{FR}\right\|}{\left\|\dot{\boldsymbol{\varepsilon}}_{pd}^{FR}\right\|} = \frac{\dot{\lambda}\,\|\mathbf{N}_v\|}{\dot{\lambda}\,\|\mathbf{N}_d\|} = \frac{\sqrt{2}}{3}\eta\alpha \tag{38}$$

being α the flow rule dilation angle coefficient, $\eta = \sigma_m/\sigma_{vm}$ the stress triaxiality, and $\|\mathbf{N}_v\|$ and $\|\mathbf{N}_d\|$ the modules of the volumetric and deviatoric flow tensor components respectively (dilation/compaction sign enforced by stress state represented by the stress triaxiality η).
The combination of equation (38) and (10) leads to:

$$\boxed{\frac{\dot{\varepsilon}_{pv}}{\dot{\varepsilon}_{peq}} = \eta\alpha} \tag{39}$$

which represents a general relationship in SAMP-1 between the volumetric and equivalent plastic strain rates, the von Mises and mean stresses (i.e. the four physical magnitudes that define the volumetric and deviatoric plastic work energetic conjugates) and the dilation angle coefficient α.
Equation (39) clearly shows the influence of the stress state in the material plastic dilation behaviour. Stress states with higher triaxialities lead to proportionally higher volumetric plastic strains development with respect to the deviatoric ones (i.e. higher $\dot{\mathcal{E}}_{\mathrm{pv}}/\dot{\mathcal{E}}_{\mathrm{peq}}$ ratio). Thus, as expected, biaxial tension conditions will generate higher $\dot{\mathcal{E}}_{\mathrm{pv}}/\dot{\mathcal{E}}_{\mathrm{peq}}$ ratio than uniaxial tension conditions.
Particularizing $\mathrm{tg}\varphi^{\mathrm{FR}}$ (Eq. 38) for the uniaxial tension case ($\eta_{\mathrm{ut}} = 1/3$) reads:

$$\mathrm{tg}\varphi_{\mathrm{ut}}^{\mathrm{FR}} = \frac{\sqrt{2}}{3}\eta_{\mathrm{ut}}\,\alpha \tag{40}$$

Recalling from section 2.1, the general expression of the dilation angle defined as a function of both the equivalent plastic strain rate and the volumetric plastic strain rate particularized for the uniaxial tension case (Eq. 11) reads:

$$\mathrm{tg}\varphi_{\mathrm{ut}} = \frac{\sqrt{2}}{3}\frac{\dot{\mathcal{E}}_{\mathrm{pv}}^{\mathrm{ut}}}{\dot{\mathcal{E}}_{\mathrm{peq}}^{\mathrm{ut}}} \tag{41}$$

Consequently, combining equations (40) and (41) the dilation angle coefficient α can be expressed as a function of measurable plastic deformations in the uniaxial tension experiments:

$$\mathrm{tg}\varphi_{\mathrm{ut}} = \mathrm{tg}\varphi_{\mathrm{ut}}^{\mathrm{FR}} \quad \Leftrightarrow \quad \alpha = \frac{\dot{\mathcal{E}}_{\mathrm{pv}}^{\mathrm{ut}}/\dot{\mathcal{E}}_{\mathrm{peq}}^{\mathrm{ut}}}{\eta_{\mathrm{ut}}} = 3\frac{\dot{\mathcal{E}}_{\mathrm{pv}}^{\mathrm{ut}}}{\dot{\mathcal{E}}_{\mathrm{peq}}^{\mathrm{ut}}} \tag{42}$$

The relationship between the plastic Poisson's ratio ν_{p} and the dilation angle coefficient α is obtained by enforcing dilation angle consistency in uniaxial stress state conditions. Thus, the dilation angle obtained from the characteristic plastic strain rate tensor in the uniaxial tension case (Eq. 13) and the one obtained from the flow rule (Eq. 40) need to agree. In other words,

$$\mathrm{tg}\varphi_{\mathrm{ut}} = \frac{\left\|\dot{\boldsymbol{\mathcal{E}}}_{\mathrm{pv}}^{\mathrm{ut}}\right\|}{\left\|\dot{\boldsymbol{\mathcal{E}}}_{\mathrm{pd}}^{\mathrm{ut}}\right\|} = \frac{1}{\sqrt{2}}\frac{1-2\nu_{\mathrm{p}}}{1+\nu_{\mathrm{p}}} \overset{\mathrm{def}}{=} \mathrm{tg}\varphi_{\mathrm{ut}}^{\mathrm{FR}} = \frac{\left\|\dot{\boldsymbol{\mathcal{E}}}_{\mathrm{pv}}^{\mathrm{FR}}|_{\mathrm{ut}}\right\|}{\left\|\dot{\boldsymbol{\mathcal{E}}}_{\mathrm{pd}}^{\mathrm{FR}}|_{\mathrm{ut}}\right\|} = \frac{\sqrt{2}}{9}\alpha \tag{43}$$

hence,

$$\mathrm{tg}\varphi_{\mathrm{ut}} \overset{\mathrm{def}}{=} \mathrm{tg}\varphi_{\mathrm{ut}}^{\mathrm{FR}} \quad \Leftrightarrow \quad \alpha = \frac{9}{2}\frac{1-2\nu_{\mathrm{p}}}{1+\nu_{\mathrm{p}}} \;\&\; \nu_{\mathrm{p}} = \frac{9-2\alpha}{18+2\alpha} \tag{44}$$

Both plastic Poisson's ratio and dilation angle coefficient expressions respect the dilation angle consistency condition. In other words,

$$\left.\begin{aligned} \alpha &= 3\frac{\dot{\mathcal{E}}_{\mathrm{pv}}^{\mathrm{ut}}}{\dot{\mathcal{E}}_{\mathrm{peq}}^{\mathrm{ut}}} \\ \nu_{\mathrm{p}} &= \frac{1}{2}\left(1-\frac{\dot{\mathcal{E}}_{\mathrm{pv}}^{\mathrm{ut}}}{\dot{\mathcal{E}}_{\mathrm{p}}^{\mathrm{ut}}}\right) \end{aligned}\right\} \Leftrightarrow \nu_{\mathrm{p}} = \frac{9-2\alpha}{18+2\alpha} \quad \& \quad \alpha = \frac{9}{2}\frac{1-2\nu_{\mathrm{p}}}{1+\nu_{\mathrm{p}}} \tag{45}$$

As a summary regarding the material dilation angle φ, dilation angle coefficient α and plastic Poisson's ratio ν_{p} in SAMP-1 and SAMP-Light:

- The dilation angle φ depends on both:
  - the stress state triaxiality η as well as;
  - the dilation angle coefficient α which is characterized in uniaxial conditions by means of the measurement of the plastic Poisson's ratio ν_{p}.

- The dilation angle coefficient α can be understood as the material plastic dilation (represented by the $\dot{\mathcal{E}}_{pv}/\dot{\mathcal{E}}_{peq}$ ratio) normalized by the stress triaxiality of the corresponding plastic loading stress state. In other words,

$$\alpha = \frac{\dot{\mathcal{E}}_{pv}/\dot{\mathcal{E}}_{peq}}{\eta} \tag{46}$$

- In uniaxial tension conditions, the dilation angle coefficient α only depends on the plastic Poisson's ratio ν_p.
- For a given yield stress surface size, both the dilation angle coefficient α and the plastic Poisson's ratio ν_p are constant for all stress states involving hydrostatic tension.
- The plastic Poisson's ratio ν_p only evolves when the yield stress surface grows (i.e. due to the plastic strain progress).
- The plastic Poisson's ratio ν_p can be defined as a function of both uniaxial tension and compression plastic strains.

The actual yield surface geometry in the principal stress space can be studied in the meridian plane diagram that relates the deviatoric stress tensor module to the hydrostatic stress tensor module ($\|\mathbf{S}\|$ and $\|\boldsymbol{\sigma}_H\|$ respectively). The latter (i.e. $\|\boldsymbol{\sigma}_H\|$) affected by the pressure sign to differentiate between hydrostatic tension and compression (i.e. $\|\boldsymbol{\sigma}_H\|^* \overset{\text{def}}{=} \|\boldsymbol{\sigma}_H\| \operatorname{sign}(p) = \sqrt{3}|p| \operatorname{sign}(p) = \sqrt{3}\, p$). In the $\|\mathbf{S}\|$-$\|\boldsymbol{\sigma}_H\|^*$ diagram the dilation angle obtained from equation (38) can be directly used to plot the growth direction of the plastic strain tensor.

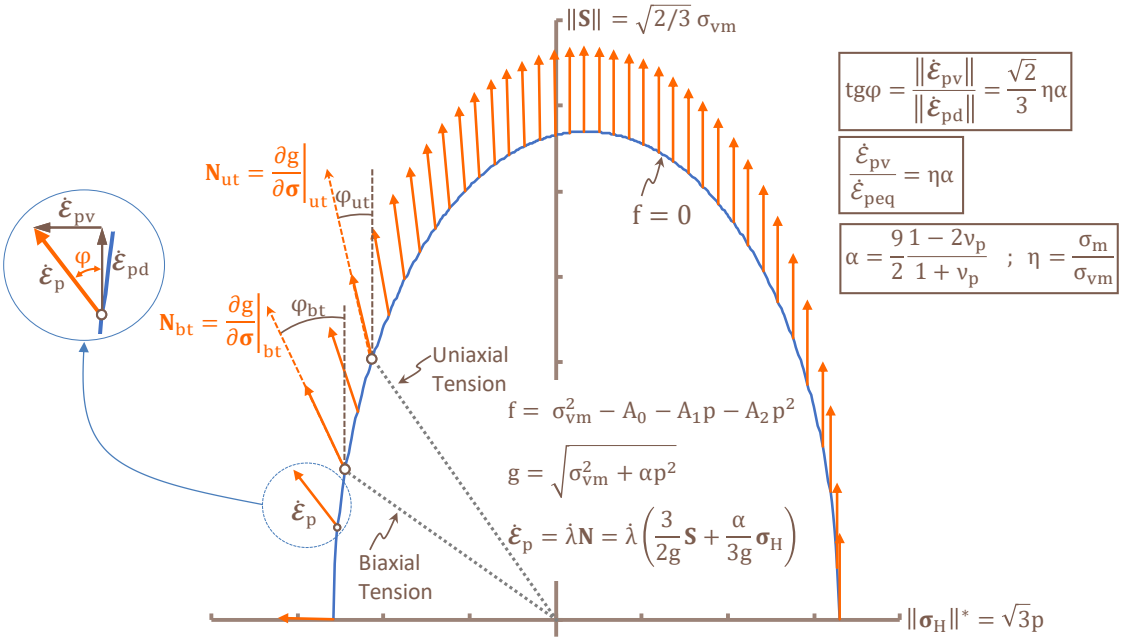

The figure above illustrates the SAMP-1 general quadratic yield surface and the plastic strain tensor growth direction imposed by SAMP-1 non-associated flow rule. Both are shown in the $\|\mathbf{S}\|$-$\|\boldsymbol{\sigma}_H\|^*$ meridian plane of the coaxial principal stress space.

The figure below illustrates the SAMP-Light linear yield surface and the plastic strain tensor growth direction imposed by SAMP-Light non-associated flow rule. Both are shown in the $\|\mathbf{S}\|$-$\|\boldsymbol{\sigma}_H\|^*$ meridian plane of the coaxial principal stress space.

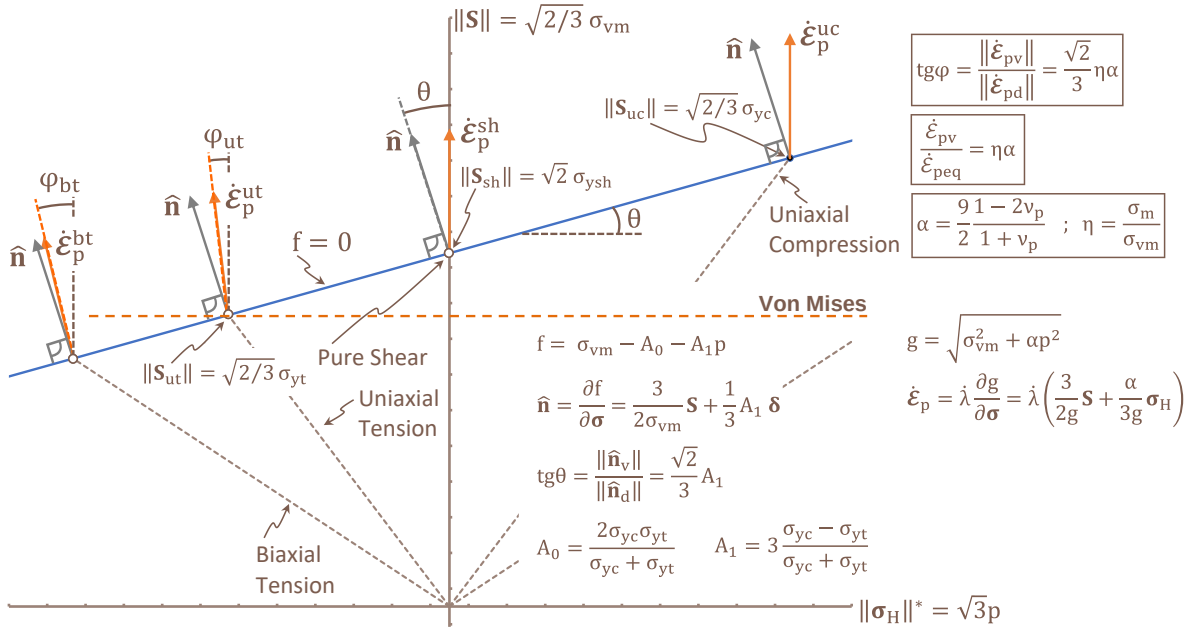

4.2 SAMP-1 and SAMP-Light experimental inputs consistency

In order to achieve a proper level of correlation and numerical stability when SAMP-1 is used, it is required to ensure the experimental inputs consistency. The combination of the expressions and relations from the previous section in uniaxial tension conditions leads to the following deviatoric and volumetric plastic strain rate tensor expressions.

$$\dot{\boldsymbol{\varepsilon}}_{pd}^{ut} = \begin{bmatrix} \dot{\varepsilon}_{peq}^{ut} & 0 & 0 \\ 0 & -\frac{1}{2}\dot{\varepsilon}_{peq}^{ut} & 0 \\ 0 & 0 & -\frac{1}{2}\dot{\varepsilon}_{peq}^{ut} \end{bmatrix} \qquad \dot{\boldsymbol{\varepsilon}}_{pv}^{ut} = \begin{bmatrix} \frac{1}{3}\dot{\varepsilon}_{pv}^{ut} & 0 & 0 \\ 0 & \frac{1}{3}\dot{\varepsilon}_{pv}^{ut} & 0 \\ 0 & 0 & \frac{1}{3}\dot{\varepsilon}_{pv}^{ut} \end{bmatrix} \quad (47)\,, \quad (48)$$

with,

$$\dot{\varepsilon}_{peq}^{ut} = \sqrt{\frac{2}{3}\dot{\boldsymbol{\varepsilon}}_{pd}^{ut} : \dot{\boldsymbol{\varepsilon}}_{pd}^{ut}} = \frac{2}{3}(1+\nu_p)\dot{\varepsilon}_p^{ut} = \dot{\varepsilon}_p^{ut} - \frac{1}{3}\dot{\varepsilon}_{pv}^{ut} \quad (49)$$

$$\dot{\varepsilon}_{pv}^{ut} = (1-2\nu_p)\dot{\boldsymbol{\varepsilon}}_p^{ut} = \dot{\varepsilon}_v^{ut} - \frac{\sigma_m^{ut}}{K} \quad (50)$$

SAMP-1 total plastic strain rate tensor expression can be directly obtained by summing up the volumetric and deviatoric plastic strain tensors above.

Obtaining from uniaxial tension experiments the volumetric-deviatoric split of both the total strain tensor ($\boldsymbol{\varepsilon}_v$ and $\boldsymbol{\varepsilon}_d$) and the plastic strain tensor ($\boldsymbol{\varepsilon}_{pv}$ and $\boldsymbol{\varepsilon}_{pd}$) allows the direct validation of the material card experimental inputs consistency in uniaxial tension conditions. Thus, the evolution of the stress and strain tensors built up from uniaxial tension experimental data should always satisfy:

$$\boldsymbol{\sigma}^{ut} = 2G\left(\boldsymbol{\varepsilon}_d^{ut} - \boldsymbol{\varepsilon}_{pd}^{ut}\right) + 3K\left(\boldsymbol{\varepsilon}_v^{ut} - \boldsymbol{\varepsilon}_{pv}^{ut}\right) = \mathbf{S}^{ut} + \boldsymbol{\sigma}_H^{ut} \quad (51)$$

The deviatoric and hydrostatic stress tensors can also be quantified from the experimentally measured engineering stress and strains.

In the SAMP-1 work frame, equation (51) imposes an additional consistent plastic Poisson's ratio expression based on experimentally measured variables already defined in this work:

$$\nu_p = -\frac{\mathcal{E}_2^{ut} + \nu\,\sigma_{ut}/E}{\mathcal{E}_1^{ut} - \sigma_{ut}/E} \tag{52}$$

which clearly reduces to the classic plastic Poisson's ratio definition:

$$\nu_p = -\frac{\mathcal{E}_{p\,trans}^{ut}}{\mathcal{E}_{p\,long}^{ut}} \tag{53}$$

Being $\mathcal{E}_{p\,long}^{ut}$ and $\mathcal{E}_{p\,trans}^{ut}$ the uniaxial tension longitudinal and transverse plastic strains respectively.

Additionally, the stress-strain user-input curves in SAMP-1 and SAMP-Light (e.g. tension, compression and shear) need to provide an overall consistent and stable convex yield stress surface growth.

Experimental inputs consistency is especially relevant for securing quality, reliability, numerical stability and reasonable computational cost of the material card when used in full vehicle crashworthiness CAE analysis.

This work shows that the consistent evaluation of the plastic Poisson's ratio based on both plasticity theory and actual physical test results is a key factor for the quality and reliability of non-isochoric material laws. The consistent approach has been fully validated for shell elements providing robust, reliable and numerically stable shell-based crashworthiness CAE analysis.

4.3 Non-isochoric plastic work in SAMP-1 and SAMP-Light

As explained in section 2.4, non-isochoric plasticity material laws consider the plastic work from both deviatoric (shear) and volumetric yielding for the computation of the material energy absorption.
Based on energy conservation principles, both von Mises and SAMP-1 plasticity models under the same monotonic plastic loading conditions must deliver the same total plastic work rate $\dot{W}_p$. In other words,

$$\dot{W}_p = \dot{W}_{pd}^{vm} + \dot{W}_{pv}^{vm} = \sigma_{vm} \cdot \dot{\mathcal{E}}_{peq}^{vm} \tag{54}$$

$$\dot{W}_p = \dot{W}_{pd}^{samp} + \dot{W}_{pv}^{samp} = \sigma_{vm} \cdot \dot{\mathcal{E}}_{peq}^{samp} + \sigma_m \cdot \dot{\mathcal{E}}_{pv}^{samp} \tag{55}$$

In the von Mises model, the total plastic work is only due to the shear plastic mechanism (i.e. $\dot{\mathcal{E}}_{pv}^{vm} = 0$) and, in SAMP-1, the total plastic work is distributed between shear and volumetric plastic mechanisms.

The combination of equations (54) and (55) leads to:

$$\dot{\mathcal{E}}_{peq}^{samp} = \dot{\mathcal{E}}_{peq}^{vm} - \eta\,\dot{\mathcal{E}}_{pv}^{samp} \quad \text{with} \quad \eta = \sigma_m/\sigma_{vm} \tag{56}$$

In the comparison between von Mises and SAMP-1 plasticity models it is important to remark that in SAMP-1 the equivalent plastic strain expression is influenced by the presence of the volumetric plastic strain. Uniaxial tension, biaxial tension and pure shear conditions will be analysed in this section to illustrate this influence.

Let $\dot{\varepsilon}_p^{bt}$ and $\dot{\varepsilon}_p^{sh}$ be the biaxial tension and pure shear plastic strain rates as defined in SAMP-1:

$$\dot{\varepsilon}_p^{bt} = \dot{\varepsilon}^{bt} - (1-\nu)\frac{\sigma_{bt}}{E} \quad , \quad \dot{\varepsilon}_p^{sh} = \dot{\varepsilon}^{sh} - \frac{\sigma_{sh}}{2G} \tag{57}$$

Let $\dot{\boldsymbol{\varepsilon}}_p^{bt}$ and $\dot{\boldsymbol{\varepsilon}}_p^{sh}$ be the SAMP-1 characteristic plastic strain rate tensors under biaxial tension and pure shear conditions and ν_p the plastic Poisson's ratio exhibited during uniaxial tension yielding:

$$\dot{\boldsymbol{\varepsilon}}_p^{bt} = \begin{bmatrix} \dot{\varepsilon}_p^{bt} & 0 & 0 \\ 0 & \dot{\varepsilon}_p^{bt} & 0 \\ 0 & 0 & -2\dfrac{\nu_p}{1-\nu_p}\,\dot{\varepsilon}_p^{bt} \end{bmatrix} \quad , \quad \dot{\boldsymbol{\varepsilon}}_p^{sh} = \begin{bmatrix} 0 & \dot{\varepsilon}_p^{sh} & 0 \\ \dot{\varepsilon}_p^{sh} & 0 & 0 \\ 0 & 0 & 0 \end{bmatrix} \tag{58}$$

The table below summarizes the expressions of the plastic work deviatoric and volumetric energetic conjugates for von Mises and SAMP-1 models under different loading conditions.

Loading condition	Von Mises stress σ_{vm}	Mean stress σ_m	Stress Triaxiality $\eta = \frac{\sigma_m}{\sigma_{vm}}$	Von Mises equivalent plastic strain $\dot{\varepsilon}_{peq}^{vm}$	SAMP equivalent plastic strain $\dot{\varepsilon}_{peq}^{samp}$	Volumetric plastic strain $\dot{\varepsilon}_{pv}$
Uniaxial tension	σ_{ut}	$\frac{1}{3}\sigma_{ut}$	$\frac{1}{3}$	$\dot{\varepsilon}_p^{ut}$	$\dot{\varepsilon}_p^{ut} - \frac{1}{3}\dot{\varepsilon}_{pv}^{ut}$ $\frac{2}{3}(1+\nu_p)\dot{\varepsilon}_p^{ut}$	$(1-2\nu_p)\dot{\varepsilon}_p^{ut}$
Biaxial tension	σ_{bt}	$\frac{2}{3}\sigma_{bt}$	$\frac{2}{3}$	$2\dot{\varepsilon}_p^{bt}$	$2\dot{\varepsilon}_p^{bt} - \frac{2}{3}\dot{\varepsilon}_{pv}^{bt}$ $\frac{2}{3}\frac{1+\nu_p}{1-\nu_p}\,\dot{\varepsilon}_p^{bt}$	$2\frac{1-2\nu_p}{1-\nu_p}\,\dot{\varepsilon}_p^{bt}$
Pure shear	$\sqrt{3}\,\sigma_{sh}$	0	0	$\frac{2}{\sqrt{3}}\dot{\varepsilon}_p^{sh}$	$\frac{2}{\sqrt{3}}\dot{\varepsilon}_p^{sh}$	0

Plastic work rates for both von Mises and SAMP-1 models under different loading conditions are summarized in the tables below.

Uniaxial Tension	Shear plastic work rate $\dot{W}_{pd} = \sigma_{vm}\,\dot{\varepsilon}_{peq}$	Volumetric plastic work rate $\dot{W}_{pv} = \sigma_m\,\dot{\varepsilon}_{pv}$	Total plastic work rate $\dot{W}_p = \dot{W}_{pd} + \dot{W}_{pv}$
Von Mises (MAT 24)	$\sigma_{ut}\,\dot{\varepsilon}_p^{ut}$	0	$\sigma_{ut}\,\dot{\varepsilon}_p^{ut}$
SAMP-1	$\sigma_{ut}\left(\dot{\varepsilon}_p^{ut} - \frac{1}{3}\dot{\varepsilon}_{pv}^{ut}\right)$	$\frac{1}{3}\sigma_{ut}\,\dot{\varepsilon}_{pv}^{ut}$	$\sigma_{ut}\,\dot{\varepsilon}_p^{ut}$

Biaxial Tension	Shear plastic work rate $\dot{W}_{pd} = \sigma_{vm}\,\dot{\varepsilon}_{peq}$	Volumetric plastic work rate $\dot{W}_{pv} = \sigma_{m}\,\dot{\varepsilon}_{pv}$	Total plastic work rate $\dot{W}_{p} = \dot{W}_{pd} + \dot{W}_{pv}$
Von Mises (MAT 24)	$\sigma_{bt}\left(2\dot{\varepsilon}_{p}^{bt}\right)$	0	$2\sigma_{bt}\,\dot{\varepsilon}_{p}^{bt}$
SAMP-1	$\sigma_{ut}\left(2\dot{\varepsilon}_{p}^{bt} - \frac{2}{3}\dot{\varepsilon}_{pv}^{bt}\right)$	$\frac{2}{3}\sigma_{bt}\,\dot{\varepsilon}_{pv}^{bt}$	$2\sigma_{bt}\,\dot{\varepsilon}_{p}^{bt}$

Pure Shear	Shear plastic work rate $\dot{W}_{pd} = \sigma_{vm}\,\dot{\varepsilon}_{peq}$	Volumetric plastic work rate $\dot{W}_{pv} = \sigma_{m}\,\dot{\varepsilon}_{pv}$	Total plastic work rate $\dot{W}_{p} = \dot{W}_{pd} + \dot{W}_{pv}$
Von Mises (MAT 24)	$\sqrt{3}\,\sigma_{sh}\frac{2}{\sqrt{3}}\dot{\varepsilon}_{p}^{sh}$	0	$2\sigma_{sh}\,\dot{\varepsilon}_{p}^{sh}$
SAMP-1	$\sqrt{3}\,\sigma_{sh}\frac{2}{\sqrt{3}}\dot{\varepsilon}_{p}^{sh}$	0	$2\sigma_{sh}\,\dot{\varepsilon}_{p}^{sh}$

Volumetric and shear plastic work split is the necessary base to develop reliable CAE models which properly predict the fracture behaviour in materials that exhibit volumetric plastic dilation from the plasticity onset.

4.4 Application on extruded aluminium and thermoplastic

This section briefly shows the benefits of using SAMP-1 material law over an extruded aluminium and a thermoplastic, both being standard automotive materials. Both materials can be considered linear elastic isotropic materials for which void nucleation and growth start with the plasticity onset. Therefore, the material yielding response can be captured with a non-isochoric material plasticity law like SAMP-1.
The pictures below show shell-based CAE results versus physical experiments. For extruded aluminium the benefits of SAMP-1 are shown based on the uniaxial tensile and pure shear tests. For the thermoplastic the benefits are shown based on uniaxial tension and dart impact tests.

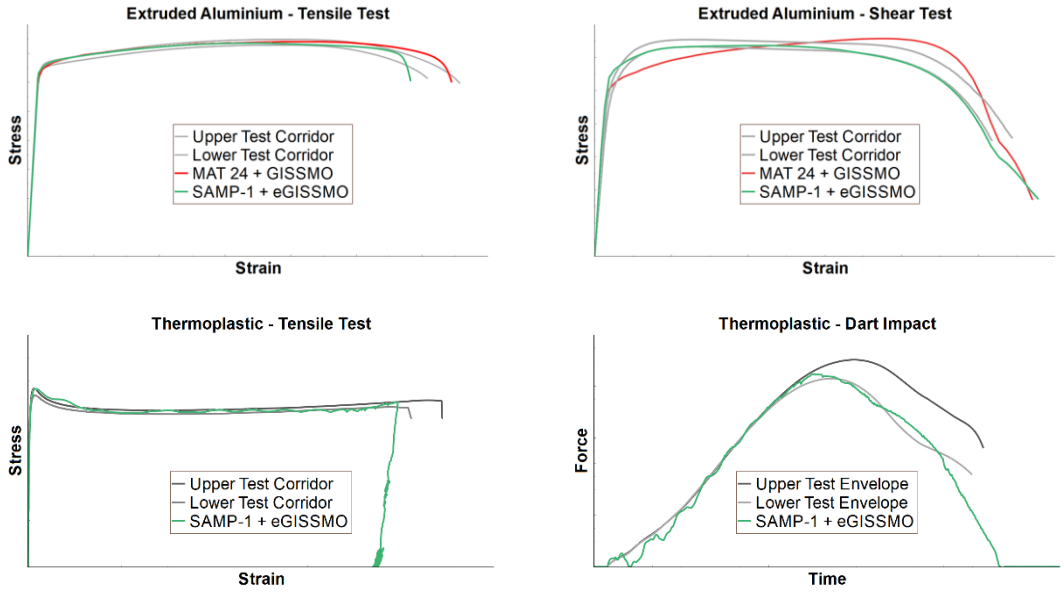

For both extruded aluminium alloys and thermoplastics in crashworthiness CAE analysis the material law needs to:

- capture the tension-shear-compression yield stress asymmetry by means of the yield stress surface shape and growth driven by tension, shear and compression plastic behaviour;
- develop the correct volumetric-deviatoric plastic strain ratio (i.e. $\dot{\varepsilon}_{\mathrm{pv}}/\dot{\varepsilon}_{\mathrm{peq}}$ ratio) by means of the non-associated plastic potential driven by the stress state triaxiality and the plastic dilation behaviour, the latter defined as a function of the plastic Poisson ratio in uniaxial tension conditions (i.e. $\dot{\varepsilon}_{\mathrm{pv}}/\dot{\varepsilon}_{\mathrm{peq}} = \eta\alpha$ with $\alpha = \mathrm{f}(\nu_{\mathrm{p}}^{\mathrm{ut}})$);
- and isotropically degrade the material properties due to both hydrostatic and shear plastic mechanisms caused by the coexisting volumetric and deviatoric stress states respectively.

The above-mentioned objectives are achieved combining SAMP-1 and eGissmo (i.e. **`*MAT_ADD_GENERALIZED_DAMAGE`**). This approach shows a proper level of correlation between shell-based CAE and experimental results for the extruded aluminium and the thermoplastic studied in this paper.
Extruded aluminium experimental results clearly show that pure shear plastic behaviour does not respect von Mises plasticity assumptions (i.e. $\sigma_{\mathrm{yield}}^{\mathrm{shear}} > \sigma_{\mathrm{yield}}^{\mathrm{tension}}/\sqrt{3}$). Therefore, a pressure-dependent yield surface is required. Material degradation due to void nucleation and growth (i.e. volumetric damage) appears in the plastic region before void coalescence and shear damage dominates the final material fracture.
In the thermoplastic case, it is important to remark that dart impact test conditions can be understood as dynamic biaxial tension conditions. Biaxial tension conditions lead to higher material plastic dilation when compared to uniaxial tension conditions due to the higher both mean stress and stress triaxiality. Therefore, the good correlation for both uniaxial tension and dart impact confirms the approach of characterizing the plastic dilation behaviour from uniaxial tension and introducing the influence of different stress states by means of the stress state triaxiality. Tension-compression yield stress asymmetry and volumetric-shear damage are also relevant material behaviours to be considered in the material card generation for thermoplastics.
The consistency and numerical stability of the shell-based material cards for the studied aluminium extrusion and thermoplastic is secured by means of the application of the approach described in previous sections.

5 Conclusions

Although classically, automotive body materials have been considered to exhibit isochoric plasticity, relevant structural materials show non-isochoric plastic behaviour. Non-isochoric plasticity can be crucial for the achievement of an efficient lightweight design where the prediction of the material crash performance and fracture needs to be robust and reliable. This paper provides a clean process to assess when body structural materials deviate from the classic isochoric plasticity assumption.
Understanding that Digital Image Correlation is today an industry standard in the uniaxial tension test setup, Non-isochoric Plasticity Assessment does not require additional experimental efforts to be applied. The necessary experimental data is already available in most OEMs material databases. NPA application over the complete material database will provide valuable information regarding the plasticity accuracy of the CAE material cards.
Once NPA is assessed, CAE engineers can decide which is the most appropriate material law based on an objective experimental data analysis.
Choosing the correct material law can result in an improvement of design lightweight efficiency of between 10% and 20% depending on the material, component geometry, manufacturing

technology and performance requirements. The accurate implementation of plasticity becomes mandatory when material fracture is a central design parameter.
A general description is provided regarding plasticity theory concepts required for the usage of non-isochoric plasticity material laws. The relation between the plastic Poisson's ratio and the plastic dilation behaviour is described to define the incorporation of the non-isochoric plastic material behaviour in SAMP-1 and SAMP-Light LS-Dyna material laws. An approach for the validation of the experimental input data consistency for both SAMP-1 and SAMP-Light material laws is also proposed.
The overall approach is finally applied and validated on an extruded aluminium and a thermoplastic showing a proper level of correlation between CAE and experimental results for shell-based FE-models.

6 Acknowledgments and remarks

The complete non-isochoric plasticity material characterization approach including advanced testing protocols and forefront CAE analysis has been jointly developed and implemented by Applus+ DatapointLabs and IDIADA to deliver accurate material characterization and material card generation for SAMP-1 and SAMP-Light.

7 Correspondence

Pablo Cruz
Senior Manager Body & Passive Safety
E-mail: Pablo.Cruz@idiada.com

8 Literature

[1] RI Borja 2013: Plasticity. Modeling & Computation
[2] EA de Souza Neto et al. 2008: Computational Methods For Plasticity. Theory And Applications.
[3] R. Hadal, R. Misra. (2004). The influence of loading rate and concurrent microstructural evolution in micrometric talc- and wollastonite-reinforced high isotactic polypropylene composites. Materials Science and Engineering: A, 374, 374–389.
[4] Chen et al 2017: Flow and fracture behavior of aluminum alloy 6082-T6 at different tensile strain rates and triaxialities.
[5] LS-Dyna manuals (2020), Livermore Software Technology Corporation.
[6] S. Kolling, A. Haufe, M. Feucht, P. Du Bois. (2005). SAMP-1: A Semi-Analytical Model for the Simulation of Polymers.
[7] M. Vogler, S. Kolling, A. Haufe. (2007). A Constitutive Model for Plastics with Piecewise Linear Yield Surface and Damage.
[8] José E. Andrade. Plasticity at Caltech.
[9] M. Helbig, E. van der Giessen, A.H. Clausen, Th. Seelig. (2016). Continuum-micromechanical modeling of distributed crazing in rubber-toughened polymers.
[10] M. Benz, J. Irslinger, M. Feucht, P. Du Bois, M. Bischoff. (2019). Development of a New Method for Strain Field Optimized Material Characterization.
[11] H. Altenbach, A. Öchsner. (2014). Plasticity of Pressure-Sensitive Materials. 10.1007/978-3-642-40945-5.
[12] J. Lubliner. (2006). Plasticity Theory.
[13] J.C. Simo, T.J.R. Hughes. (1998). Computational Inelasticity.
[14] António R. Melro. (2011). Analytical and numerical modelling of damage and fracture of advanced composites.
[15] F. Van der Meer. (2016). Micromechanical validation of a mesomodel for plasticity in composites. European Journal of Mechanics - A/Solids. 60. 10.1016/j.euromechsol.2016.06.008.

[16] C. G'Sell, F. Addiego, Frédéric, A. Dahoun, J.-M. Hiver. (2004). In-situ characterization of cavitation during the deformation of semi-crystalline polymers. Annual Technical Conference - ANTEC, Conference Proceedings. 2. 2013-2017.
[17] Drucker, D.C. (1973). Plasticity theory strength-differential (SD) phenomenon, and volume expansion in metals and plastics. Metall Mater Trans B 4, 667.
[18] Jens Kristian Holmen, Bjørn Håkon Frodal, Odd Sture Hopperstad, Tore Børvik. (2017). Strength differential effect in age hardened aluminum alloys. International Journal of Plasticity, Volume 99, Pages 144-161, ISSN 0749-6419. https://doi.org/10.1016/j.ijplas.2017.09.004.